PHYSICAL REVIEW B VOLUME 2, NUMBER 7 1 OCTOBER 1970

Crystal-Field Effects and Anomalous Susceptibility of Antiferromagnets: Application to Ce-Group-V Compounds

Yung-Li Wang*
Department of Physics, Florida State University, Tallahassee, Florida 32306
and
Bernard R. Cooper
General Electric Research and Development Center, Schenectady, New York 12301
(Received 5 June 1970)

Crystal-field effects can drastically change the temperature variation of the susceptibility in antiferromagnets. The powder inverse susceptibility need no longer increase monotonically as temperature decreases below the Néel temperature, and can have a maximum and an additional minimum. We illustrate these effects for antiferromagnetic compounds containing Ce^{3+} in an octahedral crystal field. The anomalous behavior arises because there is a range of exchange field for which the Γ_7 ground-state doublet splitting decreases with increasing field until the doublet levels cross. The maximum in the powder inverse susceptibility can occur because the decrease in energy splitting leads to a rapid increase of the transverse susceptibility with decreasing temperature, and this outweighs the decrease in the longitudinal susceptibility. Our model leads to the expectation of approximately normal susceptibility behavior at low and high values of the ratio of exchange to crystal-field strength, i.e., where the doublet splitting increases with increasing exchange field. It shows anomalous behavior in the intermediate region where the splitting decreases with increasing exchange field. Since the exchange field increases with decreasing temperature, the ratio of the exchange field to crystal-field strength increases with decreasing temperature. For a certain range of exchange and crystal-field parameters, this can lead to a change from anomalous to normal energy level and susceptibility behavior with decreasing temperature. This return to normal behavior gives rise to an upturn (i.e., a second minimum) in the polycrystalline inverse susceptibility at low temperature. The behavior of the Ce-group-V compounds of NaCl structure covers the entire range of the ratio of crystal-field strength to exchange interaction. Corresponding to this variation, the susceptibility behavior is normal for the light compounds (CeP and CeAs), most anomalous for CeSb, and returns toward normal for CeBi.

I. INTRODUCTION

For antiferromagnetic materials where the crystal-field interaction is comparable to the exchange interaction, the temperature dependence of the susceptibility in the antiferromagnetic state can be quite different from that usual for antiferromagnetic materials.

As is well known, the usual behavior of the susceptibility in a simple antiferromagnet below the Néel temperature is that the transverse (to the sublattice magnetization) susceptibility is essentially constant, and the longitudinal susceptibility decreases monotonically to zero. In the usual form of display, a plot of inverse susceptibility versus temperature for a powder (i.e., polycrystalline) sample thus gives an inverse susceptibility that goes through a minimum at the Néel temperature and increases monotonically with decreasing temperature.

In this paper, we show that the crystal-field effects can drastically change the susceptibility behavior. Indeed, the inverse susceptibility need no longer increase monotonically as temperature decreases below the Néel temperature, and can have a maximum and an additional minimum. For definiteness, we have calculated the susceptibility of a cerium ion acted upon by both a cubic crystal field and a molecular exchange field. The possibility of anomalous behavior arises when the crystal-field-only ground state is the Γ_7 doublet. (The crystal-field excited state then is a Γ_8 quartet at some energy Δ.) For small effective field, the doublet splits in a normal way, energy splitting increasing with increasing field. However, as the energy equivalent of the effective field becomes comparable to the crystal-field splitting, the admixture effects from the excited quartet (i.e., the induced moment effect[1]) becomes very strong. This leads to a decrease of the doublet energy splitting with increasing effective field. Ultimately the levels cross, and for exchange fields large compared to Δ, the doublet energy splitting again increases in a normal way. Basically, the possibility of anomalous susceptibility behavior arises when the ratio of exchange energy to crystal-field

energy falls in the range where the doublet splitting decreases with increasing effective field. (There is no corresponding anomalous behavior when the ordering of the crystal-field levels is reversed, and the quartet is the ground state.) In particular, we show that the anomalous decrease of the inverse susceptibility with decreasing temperature for some range of temperature below the Néel temperature mainly arises from the rapid increase of the transverse susceptibility which outweighs the decrease of the longitudinal susceptibility; and the increase in transverse susceptibility can be traced to the crossing of the two doublet levels in an increasing molecular field.

We use our model to discuss the susceptibility behavior for Ce–group-V compounds of NaCl crystal structure.[2–5] (We omit discussion of CeN, the behavior of which is anomalous[6] in comparison both to the other rare-earth nitrides and to the heavier Ce–group-V compounds.) Here the crystal-field splitting[7–10] for the ground-state multiplet of the Ce^{3+} ion ranges from about 200 °K for CeP to approximately 20 °K or less for CeBi, and the Néel temperature[2,3] ranges from 8 °K for CeAs and 10 °K for CeP to 25 °K for CeBi. The behavior of this family of compounds then covers the entire range of the ratio of crystal-field strength to exchange interaction. CeP and CeAs are compounds with large crystal-field splitting. The molecular field is much smaller than the field where the doublet level crossing occurs. Therefore we expect a normal temperature variation of the antiferromagnetic susceptibility. For CeSb the crystal field is comparable to the exchange field, so that the anomalous susceptibility behavior associated with the level crossing is most pronounced. The final compound in the group CeBi shows a smaller crystal-field splitting (~ 20 °K) and a rather high Néel temperature (25 °K). Although the anomalous behavior persists, the decrease of inverse susceptibility as T decreases, as predicted by the theory, is less pronounced than for CeSb. Unfortunately, the detailed behavior of the magnetic structures of CeSb and CeBi is not known, although there is evidence in both cases for the development of a noncollinear structure.[8,11] Since neutron diffraction experiments[8] show that CeAs has type-I antiferromagnetic ordering (and presumably the same is true for CeP), for illustrative purposes we assume the same magnetic structure in the calculations for CeSb and CeBi. Although the noncollinearity may have certain effects on the susceptibility behavior for CeSb and CeBi, we suggest that the doublet-energy-level crossing effect is the predominant factor in the observed behavior. This supposition is supported by a fairly good fit of the experimental data with reasonable parameters.

In Sec. II we discuss the nature of the eigenfunctions and energy levels of a Ce^{3+} ion under the combined influence of a cubic crystal field (also allowing for a tetragonal distortion[12]) and an exchange molecular field. The transverse and longitudinal susceptibilities in the antiferromagnetically ordered phase are calculated in Sec. III. In Sec. IV we discuss in detail the crystal-field effects on the behavior of the magnetic susceptibilities; and in Sec. V, we apply the theory to study the susceptibilities of the Ce–group-V compounds.

II. ENERGY LEVELS OF Ce^{3+} IONS UNDER COMBINED EFFECT OF CUBIC CRYSTAL FIELD AND EFFECTIVE EXCHANGE FIELD

In this section we consider the energy eigenfunctions and eigenvalues of a Ce^{3+} ion under the combined effect of cubic crystal field and an exchange molecular field. (For later convenience in the discussion of the cerium compounds, we also include the possibility of a tetragonal distortion. Our discussion of the detailed energy-level behavior in the latter part of this section is, however, for simplicity restricted to the purely cubic case. For a small tetragonal distortion, the essential characteristics of the energy-level scheme are not altered.)

In a cubic crystal field (with tetragonal distortion) plus a molecular field, the effective Hamiltonian for a Ce^{3+} ion is

$$H = B_4(O_4^0 + 5O_4^4) + B_2 O_2^0 - g\mu_B H_m J_z \,. \tag{2.1}$$

Here we have taken the z axis as a $\langle 001\rangle$ crystal axis parallel to the direction of magnetic ordering. The cubic crystal-field operators are

$$O_4^0 \equiv 35J_z^4 - 30J(J+1)J_z^2 + 25J_z^2 - 6J(J+1) + 3J^2(J+1)^2 \,, \tag{2.2a}$$

$$O_4^4 \equiv \tfrac{1}{2}(J_+^4 + J_-^4) \,. \tag{2.2b}$$

The additional crystal-field term O_2^0 arises in the presence of a tetragonal distortion:

$$O_2^0 \equiv 3J_z^2 - J(J+1) \,. \tag{2.3}$$

In Eq. (2.1), H_m denotes the molecular field acting on a given Ce^{3+} ion.

In the absence of exchange and distortion, the crystal-field states are a Γ_7 doublet and a Γ_8 quartet with a splitting Δ,

$$\Delta = 360B_4 \,. \tag{2.4}$$

For positive B_4, the ground state is the doublet.

Defining

$$h_m \equiv g\mu_B H_m / B_4 \tag{2.5a}$$

and

$$\delta \equiv B_2/B_4 \,, \tag{2.5b}$$

the eigenstates and corresponding energy eigenvalues for the Hamiltonian of (2.1) are given by

$$\psi_1 = -\sin\theta\left|-\tfrac{5}{2}\right\rangle + \cos\theta\left|\tfrac{3}{2}\right\rangle , \quad (2.6a)$$

$$\psi_2 = -\sin\phi\left|\tfrac{5}{2}\right\rangle + \cos\phi\left|-\tfrac{3}{2}\right\rangle , \quad (2.6b)$$

$$\psi_3 = \cos\theta\left|-\tfrac{5}{2}\right\rangle + \sin\theta\left|\tfrac{3}{2}\right\rangle , \quad (2.6c)$$

$$\psi_4 = \cos\phi\left|\tfrac{5}{2}\right\rangle + \sin\phi\left|-\tfrac{3}{2}\right\rangle , \quad (2.6d)$$

$$\psi_5 = \left|\tfrac{1}{2}\right\rangle , \quad (2.6e)$$

$$\psi_6 = \left|-\tfrac{1}{2}\right\rangle , \quad (2.6f)$$

with

$$\tan 2\theta = 30(\sqrt{5})/(60 + 3\delta + h_m) , \quad (2.7a)$$

$$\tan 2\phi = 30(\sqrt{5})/(60 + 3\delta - h_m) . \quad (2.7b)$$

(Here $J=\frac{5}{2}$ for Ce^{3+}, and we have labeled the states on the right in Eqs. (2.6) by their J_z quantum numbers.)

The energy eigenvalues corresponding to the eigenstates in Eq. (2.6) are

$$E_1 = E(-\tfrac{5}{2})\sin^2\theta + E(\tfrac{3}{2})\cos^2\theta - 60(\sqrt{5})\sin 2\theta, \quad (2.8a)$$

$$E_2 = E(\tfrac{5}{2})\sin^2\theta + E(-\tfrac{3}{2})\cos^2\phi - 60(\sqrt{5})\sin 2\phi , \quad (2.8b)$$

$$E_3 = E(-\tfrac{5}{2})\cos^2\phi + E(\tfrac{3}{2})\sin^2\theta + 60(\sqrt{5})\sin 2\theta , \quad (2.8c)$$

$$E_4 = E(\tfrac{5}{2})\cos^2\phi + E(-\tfrac{3}{2})\sin^2\phi + 60(\sqrt{5})\sin 2\phi , \quad (2.8d)$$

$$E_5 = E(\tfrac{1}{2}) , \quad (2.8e)$$

$$E_6 = E(-\tfrac{1}{2}), \quad (2.8f)$$

where we define

$$E(\pm\tfrac{5}{2}) \equiv B_4(60 + 10\delta \mp 5/2h_m) , \quad (2.9a)$$

$$E(\pm\tfrac{3}{2}) \equiv B_4(-180 - 2\delta \mp 3/2h_m) , \quad (2.9b)$$

$$E(\pm\tfrac{1}{2}) \equiv B_4(120 - 8\delta \mp 1/2h_m) . \quad (2.9c)$$

In the absence of distortion and of exchange interaction, the states described by Eqs. (2.6) and (2.8) reduce to the crystal-field-only states. For $B_4 > 0$, the crystal-field-only ground state is the Γ_7 doublet for which the wave functions are

$$\psi^0_{1,2} = (\sqrt{\tfrac{5}{6}})\left|\pm\tfrac{3}{2}\right\rangle - (\sqrt{\tfrac{1}{6}})\left|\mp\tfrac{5}{2}\right\rangle , \quad (2.10)$$

with magnetic moment $\mp\frac{5}{6}g\mu_B$ ($g=\frac{6}{7}$). This magnetic moment is much smaller than the free-ion moment $2.5g\mu_B$. However, as the molecular field increases from zero, the wave functions of the excited states mix into the ground-state doublet and the magnetic moment of the ground state can be drastically changed.

The change in the energy-level structure, corresponding to this mixing of wave functions, as the molecular field increases plays a key role in the susceptibility behavior which we shall discuss below. This variation of energy (in units of B_4) is given in Fig. 1. The initial slope for E_2 is $+\frac{5}{6}$, corresponding to the moment of the purely Γ_7 crystal-field state. However, with increasing molecular field, because of the admixture from the crystal-field excited quartet, the $J_z = +\frac{5}{2}$ component of ψ_2 increases. As shown in Fig. 2, this leads to a decrease of the slope until the slope goes to zero at $h_m \simeq 40$, beyond which E_2 decreases with increasing effective field as the magnetic moment of ψ_2 becomes positive. As the moment for the ψ_2 level approaches its saturation value of $\frac{5}{2}g\mu_B$ with increasing h_m, the energy E_2 decreases more rapidly than does E_1 (the moment of ψ_1 saturates at $\frac{3}{2}g\mu_B$); and the energy E_2 crosses below E_1 at $h_m = 230$. As we shall show later, this crossing of the ground-state doublet levels is the source of the anomalous behavior possible for the magnetic susceptibilities and magnetizations of Ce^{3+} compounds.

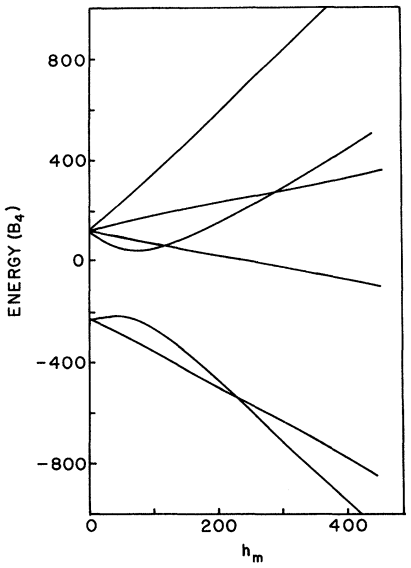

FIG. 1. Energy-level variation with molecular field for a Ce^{3+} ion in a cubic crystal field. The energy is in units of B_4, the crystal-field parameter, and $h_m \equiv g\mu_B H_m/B_4$ gives the molecular field in dimensionless form.

If the sign of B_4 is reversed (i.e., $B_4 < 0$), the Γ_8 crystal-field quartet lies lower than the Γ_7 doublet, and there is no level crossing of the two lowest energy states in the presence of the molecular field. The susceptibilities thus behave normally.

III. THEORY OF SUSCEPTIBILITIES INCLUDING CRYSTAL FIELD

A. Longitudinal Susceptibility

In order to calculate the longitudinal susceptibility, we now consider the effect of a small applied

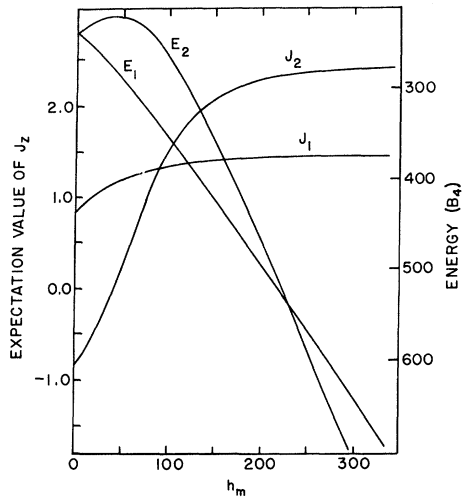

FIG. 2. Energy variation (in units of B_4), and corresponding change in magnetic moment (in units of $g\mu_B$), with increasing molecular field (in dimensionless form, $h_m \equiv g\mu_B H_m/B_4$) for ground-state crystal-field doublet of of Ce^{3+}.

magnetic field, h, along the direction of magnetization.

Let J_i, E_i and J_i', E_i' be the expectation values of J_z and energy of the ith state, respectively, before and after the application of the external field h. Then

$$\chi_{\parallel} = \lim_{h\to 0} (g\mu_B/h)[(\textstyle\sum_i J_i' e^{-E_i'/kT}/\sum_i e^{-E_i'/kT}) - (\sum_i J_i e^{-E_i/kT}/\sum_i e^{-E_i/kT})] , \quad (3.1)$$

where the summation is over all the energy eigenstates. [These are the states, given by Eqs. (2.6) and (2.8) for $h=0$, which include the effects of both the crystal field and the molecular field.]

Considering the external field as a perturbation, to the first order in h we obtain

$$E_i' = E_i - g\mu_B J_i(1+\bar{\lambda}\chi_{\parallel})h , \quad (3.2)$$

$$J_i' = J_i + 2g\mu_B h(1+\bar{\lambda}\chi_{\parallel}) \sum_j \frac{|\langle\psi_i|J_z|\psi_j\rangle|^2}{E_i - E_j} . \quad (3.3)$$

The enhancement factor $(1+\bar{\lambda}\chi_{\parallel})$ enters because the moment induced by the applied field, $\chi_{\parallel}h$, in turn produces an effective field $\bar{\lambda}\chi_{\parallel}h$ on the ion. The total effective incremental field is therefore $(1+\bar{\lambda}\chi_{\parallel})h$. Here $\bar{\lambda}$ is the paramagnetic molecular field constant for an fcc lattice:

$$\bar{\lambda} = 12\bar{\lambda}_1 + 6\lambda_2 , \quad (3.4)$$

where λ_1 and λ_2 are the molecular field coefficients giving the effective field exerted on a spin by each of its nearest neighbors and next-nearest neighbors, respectively.[13] As discussed below, $\bar{\lambda}$ is related to the paramagnetic Curie temperature.

To obtain $\chi_{\parallel}$, we substitute Eqs. (3.2) and (3.3) into (3.1):

$$\chi_{\parallel} = \chi_{\parallel}^0/(1-\bar{\lambda}\chi_{\parallel}^0) , \quad (3.5)$$

with

$$\chi_{\parallel}^0 = (g^2\mu_B^2/kT)[(\textstyle\sum_n J_n^2 e^{-E_n/kT}/\sum_n e^{-E_n/kT}) - (\sum_n J_n e^{-E_n/kT}/\sum_n e^{-E_n/kT})^2] + 2g^2\mu_B^2 \sum_{m,n\,(m\neq n)} \frac{|\langle m|J_z|n\rangle|^2}{E_m - E_n} e^{-E_n/kT} \Big/ \sum_n e^{-E_n/kT} . \quad (3.6)$$

The first two terms of $\chi_{\parallel}^0$ give the familiar expression for the longitudinal susceptibility of a spin system which has a permanent moment $g\mu_B J_n$ associated with each of the n energy levels. The last term is peculiar to the induced moment system. It reflects the change in the magnitude of moment associated with each state caused by an applied magnetic field.

B. Transverse Susceptibility

If a small external magnetic field h is applied to the system in the direction transverse to the magnetic ordering, a moment $\chi_{\perp}h$ is induced in that direction. Taking into account the enhancement effect mentioned in Sec. III A, the total incremental field is $h(1+\bar{\lambda}\chi_{\perp})$, where $\chi_{\perp}$ is the transverse susceptibility, and $\bar{\lambda}$ is the molecular field constant which is given by Eq. (3.4).

The perturbation brought about by the applied field is

$$H' = -g\mu_B h(1+\bar{\lambda}\chi_{\perp})\textstyle\sum_i J_{ix} , \quad (3.7)$$

and the perturbed states are

$$|n'\rangle = |n\rangle + \sum_{m(m\neq n)} \frac{g\mu_B h(1+\bar{\lambda}\chi_{\perp})\langle m|J_x|n\rangle\,|m\rangle}{E_m - E_n} . \quad (3.8)$$

The transverse susceptibility is then

$$\chi_{\perp} = \lim_{h\to 0} (1/h) g\mu_B \sum_{n'} \langle n'|J_x|n'\rangle\, e^{-E_{n'}/kT} / \sum_{n'} e^{-E_{n'}/kT} , \quad (3.9)$$

where $E_{n'}$ is the energy of the perturbed state n,

$$E_{n'} = E_n - g\mu_B h(1+\bar{\lambda}\chi_{\perp})\langle n|J_x|n\rangle . \quad (3.10)$$

However, $\langle n|J_x|n\rangle = 0$ in a cubic crystal field, so Eq. (3.8) is simplified to

$$\chi_{\perp} = \frac{\chi_{\perp}^0}{1-\bar{\lambda}\chi_{\perp}^0} , \quad (3.11)$$

with

$$\chi_{\perp}^{0} = 2g^2\mu_B^2 \sum_{m,n(m\neq n)} \frac{|\langle m|J_x|n\rangle|^2}{E_m - E_n} e^{-E_n/kT} \Big/ \sum_n e^{-E_n/kT}. \tag{3.12}$$

The matrix elements $\langle m|J_x|n\rangle$ are easily calculated with the wave functions given in Eq. (2.6).

C. Paramagnetic Susceptibility

Although our main interest is in the magnetically ordered regime, for completeness we give the expression for the paramagnetic susceptibility of Ce^{3+} in a cubic crystal field. This is actually the limiting case of $\chi_{\parallel}$ calculated above as the molecular field vanishes.

The paramagnetic susceptibility is

$$\chi_p = \chi_p^0/(1 - \bar{\lambda}\chi_p^0) , \tag{3.13}$$

with

$$\chi_p^0 = g^2\mu_B^2 \left(\frac{25}{36}\frac{1}{kT} + \frac{65}{18kT} e^{-\Delta/kT} + \frac{40}{9}\frac{1}{\Delta}(1 - e^{-\Delta/kT}) \right) \Big/ (1 + 2e^{-\Delta/kT}) , \tag{3.14}$$

where, as previously, Δ is the crystal-field splitting between the Γ_7 doublet and the Γ_8 quartet.

For $kT \gg \Delta$,

$$\chi_p \to C_M/(T - \bar{\lambda}C_M) = C_M/(T - \theta) , \tag{3.15}$$

with

$$C_M = \tfrac{35}{12} g^2\mu_B^2/k . \tag{3.16}$$

We now identify $\bar{\lambda}C_M$ as the paramagnetic Curie temperature. Extrapolation of the high-temperature behavior of $1/\chi_p$ thus yields the value of $\bar{\lambda}$, and this can be used in the ordered phase if there is no distortion on ordering.

IV. CRYSTAL-FIELD EFFECTS ON TEMPERATURE BEHAVIOR OF SUSCEPTIBILITIES

For the Ce–group-V compounds of NaCl structure, the susceptibility measurements have been done on powder samples. The observed susceptibility is then,

$$\chi = \tfrac{1}{3}\chi_{\parallel} + \tfrac{2}{3}\chi_{\perp} . \tag{4.1}$$

To illustrate the crystal-field effects we have calculated $1/\chi(T)$ in the antiferromagnetic phase by setting $T_N = 20\ ^\circ\mathrm{K}$ and allowing the crystal-field splitting Δ to vary from a value small compared to T_N to a value large compared to T_N. The molecular field is determined self-consistently in the usual way.[13]

In Fig. 3, we have plotted $1/\chi$ versus T for Ce^{3+} in a type-I antiferromagnet (fcc crystal structure) as Δ increases from 2 to 300 °K with $T_N = 20\ ^\circ\mathrm{K}$. Since the paramagnetic Curie temperature in a particular compound can be either positive, negative, or zero depending upon the details of the exchange interaction, in our illustrative calculations of Fig. 3 we have set $\theta = 0$.

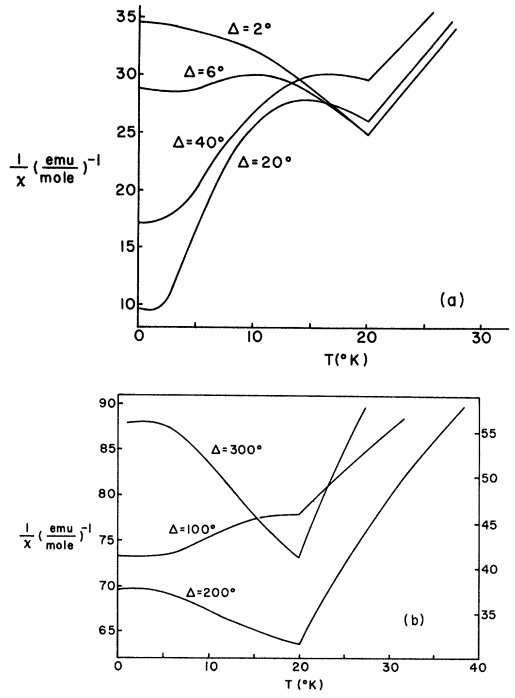

FIG. 3. Inverse susceptibility [in (emu/mole)$^{-1}$] versus temperature with fixed $T_N = 20\ ^\circ\mathrm{K}$, $\Theta = 0\ ^\circ\mathrm{K}$, and varying crystal-field splitting Δ (in °K) between the Γ_7 doublet and Γ_8 quartet. (a) shows $1/\chi$ for Δ up to 40 °K and (b) shows $1/\chi$ for larger Δ.

For small crystal field ($\Delta = 2\ ^\circ\mathrm{K}$), $\chi(T)$ behaves normally as for a simple antiferromagnet, viz., $1/\chi$ increases monotonically with decreasing temperature below the Néel temperature. As Δ increases, a downward dip in $1/\chi$ develops at low temperature and moves toward higher temperature. At $\Delta = 6\ ^\circ\mathrm{K}$, a maximum in the $1/\chi$ curve at $T = 10\ ^\circ\mathrm{K}$ and a minimum at $T = 4\ ^\circ\mathrm{K}$ become pronounced. As Δ continues to increase, the low-temperature tail of $1/\chi$ flattens out and bends downward, and the low-temperature minimum moves toward zero temperature and disappears. On the other hand, as Δ increases to values comparable to T_N, the decrease of $1/\chi$ for temperatures below its maximum becomes very large. This is shown by the $\Delta = 20\ ^\circ\mathrm{K}$ curve in Fig. 3(a).

The general type of behavior occurring for Δ comparable to T_N, a maximum in $1/\chi$ decreasing rather sharply below the temperature of the maximum, persists to values of Δ rather large compared to T_N. The low-temperature tail, however, moves up, and at $\Delta = 100\ ^\circ\mathrm{K}$ it is so flat that the

curve of $1/\chi$ versus T looks roughly like two straight lines of different slopes joining at T_N. For large enough Δ, $1/\chi(T)$ returns to the normal behavior as shown in Fig. 3(b) for $\Delta = 200\,^\circ$K and $\Delta = 300\,^\circ$K.

The variations in the behavior of $1/\chi(T)$ described above and shown in Fig. 3 can all be traced to the effects of the doublet energy-level crossing on the transverse susceptibility. To understand this, we review briefly the molecular field theory of the transverse susceptibility of a simple antiferromagnet. For simplicity we assume $S = \frac{1}{2}$.

In the molecular field, $H_m = \lambda \langle M \rangle$, the energy gap between the two levels is

$$\epsilon \equiv g\mu_B H_m = g\mu_B \lambda \langle M \rangle \ , \tag{4.2}$$

and the sublattice magnetization $\langle M \rangle$ is

$$\langle M \rangle = \tfrac{1}{2} g\mu_B (1 - e^{-\epsilon/kT})/(1 + e^{-\epsilon/kT}) \ . \tag{4.3}$$

The transverse susceptibility is

$$\chi_\perp = \frac{\chi_\perp^0}{1 - \lambda \chi_\perp^0} \ , \tag{4.4}$$

with

$$\chi_\perp^0 = 2g^2\mu_B^2 \frac{|\langle \tfrac{1}{2}|S_x|-\tfrac{1}{2}\rangle|^2}{\epsilon} \frac{(1 - e^{-\epsilon/kT})}{(1 + e^{-\epsilon/kT})}$$

$$= \tfrac{1}{2} g^2\mu_B^2 \frac{1}{\epsilon} \frac{(1 - e^{-\epsilon/kT})}{(1 + e^{-\epsilon/kT})} \ . \tag{4.5}$$

Now as temperature decreases, the population factor in Eq. (4.5) (which is proportional to the sublattice magnetization) increases. However, the energy gap ϵ increases at exactly the same rate proportional to the sublattice magnetization, and thus cancels the change in the population factor. Therefore, $\chi_\perp$ remains constant below the Néel temperature.

The longitudinal susceptibility, on the other hand, decreases as temperature decreases. This is easily seen from Eq. (3.6) with $J_n = \pm\frac{1}{2}$ and with the last term (corresponding to the induced moment effect) dropped. We obtain

$$\chi_\parallel^0 = (g^2\mu_B^2/kT)\, e^{-\epsilon/kT}/(1 + e^{-\epsilon/kT})^2 \ . \tag{4.6}$$

Thus, for the simple $S = \frac{1}{2}$ system without induced moment effects, the total susceptibility as given by Eq. (4.1) decreases as temperature decreases.

As already mentioned, the anomalous behavior of χ for Ce^{3+} compounds, is mainly due to the anomalous behavior of $\chi_\perp(T)$ in the crystal field. (There are induced moment effects on the longitudinal susceptibility. Indeed, the induced moment term in $\chi_\parallel$ becomes the major part of $\chi_\parallel$ at low temperature. However, in general these effects do not change the temperature variation of $\chi_\parallel$ from the normal behavior. That is, $\chi_\parallel$ increases as T increases, mainly because the off-diagonal elements of J_z between the molecular field states increase as the molecular field decreases.)

We therefore focus our attention on the behavior of $\chi_\perp(T)$. Because of the energy-level crossing of the Γ_7 doublet in the molecular field, $\chi_\perp(T)$ can be a sharply rising function as T decreases. It is this increase of $\chi_\perp$ which outweighs the decrease of $\chi_\parallel$ that brings about the anomalous increase of the powder χ with decreasing temperature.

Comparing the energy-level scheme of Fig. 1 with the behavior for the simple system of spin $\frac{1}{2}$ discussed above, it is clear that the peculiarity for Ce^{3+} in the crystal field is that the energy gap between the two lowest levels *decreases* as the molecular field *increases* from $h_m \simeq 90$ to the crossing at $h_m = 230$. This is in striking contrast to the usual picture of an increasing energy gap as molecular field increases. We now give a fairly detailed discussion as to how this energy-level behavior leads to the various representative types of behavior shown in Fig. 3.

The anomaly in χ versus T is most pronounced for $\Delta \simeq kT_N$. The self-consistent molecular field has been calculated, and as shown in Fig. 4, for a substantial range of temperature below T_N, is close to the value at which the doublet levels cross. Therefore the energy gap between the two levels is very small. For $\Delta = kT_N = 20^\circ$, for example (as shown in Fig. 5), for T from 5 to 14 °K the energy gap is less than 1.5 °K. It is the fact that the energy gap is both essentially independent of temperature and small compared to temperature over a significant range of temperature that leads to the increase of $\chi_\perp$ with decreasing temperature within that range. This can be seen by isolating the con-

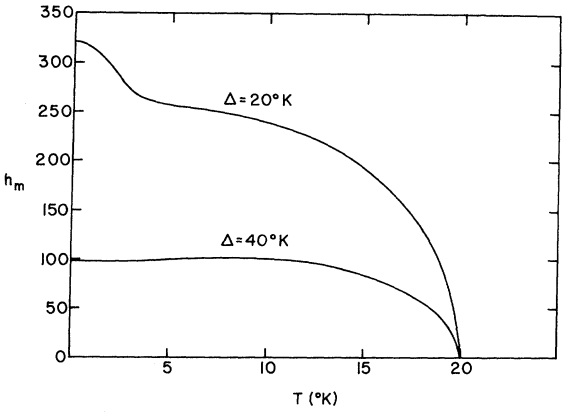

FIG. 4. Molecular field as a function of temperature for $T_N = 20\,^\circ$K with $\Delta = 20\,^\circ$K and $\Delta = 40\,^\circ$K. For $\Delta = 40\,^\circ$K, the molecular field is almost constant over a wide range of temperature.

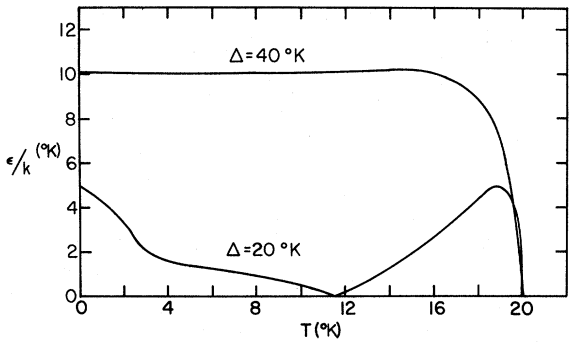

FIG. 5. Energy gap (in °K) between the two lowest energy levels as function of temperature for $T_N = 20$ °K with $\Delta = 20$ °K and $\Delta = 40$ °K.

tribution of the doublet to the total transverse susceptibility. The contribution of the doublet to χ_1^0 of Eq. (3.12) is given by

$$\chi_{12}^0 = (\chi_1^0 + \chi_2^0 e^{-\epsilon/kT})/(1 + e^{-\epsilon/kT}) , \tag{4.7}$$

with

$$\chi_1^0 \equiv a/\epsilon + \delta_1 , \tag{4.8a}$$

$$\chi_2^0 \equiv -a/\epsilon + \delta_2 , \tag{4.8b}$$

$$\epsilon \equiv E_2 - E_1 , \tag{4.9}$$

$$a \equiv 2g^2\mu_B^2 |\langle \psi_1 | J_x | \psi_2 \rangle|^2 , \tag{4.10}$$

$$\delta_{1,2} \equiv 2g^2\mu_B^2 \sum_{n(n\neq 1,2)} |\langle \psi_{1,2} | J_x | \psi_n \rangle|^2/(E_n - E_{1,2}) . \tag{4.11}$$

At temperatures low compared to the splitting between the doublet and quartet, χ_{12}^0 dominates the over-all behavior of $\chi_\perp$. When ϵ is small compared to T and essentially constant,

$$\chi_{12}^0 \simeq a/2kT + \tfrac{1}{2}(\delta_1 + \delta_2). \tag{4.12}$$

Here a, δ_1, and δ_2 are slowly varying functions of T, so that χ_{12}^0 and hence $\chi_\perp(T)$ increases with decreasing T. This is shown in Fig. 6 where $\chi_\perp$ and $\chi_\parallel$ are plotted as functions of temperature.

For Δ small compared with kT_N, the low-temperature self-consistent molecular field is much larger than the value for which the doublet levels cross. The susceptibility behavior at these temperatures is then close to that for the simple system with no crystal field present. The small upturned tail in $1/\chi$ below $T = 4$ °K for $\Delta = 6$ °K in Fig. 3 shows this tendency. As is also shown in Fig. 3 for $\Delta = 2$ °K, the susceptibility behavior becomes normal for all temperatures for very small crystal field as expected.

On the other hand, for $\Delta \gtrsim kT_N$, the molecular field at $T = 0$ °K is to the left of the value for which the level crossing occurs in Fig. 1. The magnetization at low temperatures is given by the doublet only,

$$\langle M \rangle = (\mu_1 + \mu_2 e^{-\epsilon/kT})/(1 + e^{-\epsilon/kT}) . \tag{4.13}$$

Here μ_1 and μ_2 are the moments of the Γ_7 levels in the molecular field, and $\mu_1 < \mu_2$ if the molecular field H_m is not too far from the value for level crossing (more precisely for $h_m > 90$). As we discussed earlier, in this regime, the energy gap ϵ decreases as H_m increases. As a result, as temperature rises from zero, $\langle M \rangle$ gradually grows until the temperature is high enough to populate the higher-lying levels. For further increase in temperature, the tendency to populate the higher-lying levels tends to reduce the molecular field. On the other hand, the fact that the energy gap increases with decreasing molecular field tends to cancel this effect. Because of these competing effects, for a wide range of temperature the molecular field remains essentially unchanged. As shown in Fig. 4, with $\Delta = 40$ °K, for example, the molecular field varies from $h_m = 99$ at $T = 0$ °K to 102 at 8 °K and back to 98 at 12 °K. The energy gap between the two lowest levels therefore also remains essentially constant (approximately 10 °K). This is shown in Fig. 5. The other energy levels are at least 45 °K above the ground levels and their contribution to the susceptibility can be neglected. According to Eq. (4.7), χ_{12}^0 and therefore $\chi_\perp$ increases with decreasing temperature. A plot of $\chi_\perp$ (and $\chi_\parallel$) for the case of $\Delta = 40$ °K is shown in Fig. 5. The net increase of $1/\chi$ for decreasing T for the same case ($\Delta = 40$ °K) is shown in Fig. 3(a).

As Δ assumes larger values, the molecular field moves to the left in Figs. 1 and 2 until h_m (at $T = 0$) $\lesssim 40$ whereupon $1/\chi(T)$ returns to normal behavior (as shown in Fig. 2, $h_m \simeq 40$ is where the moment of ψ_1 becomes positive). In the region $h_m < 40$, the low-lying doublet levels show energy

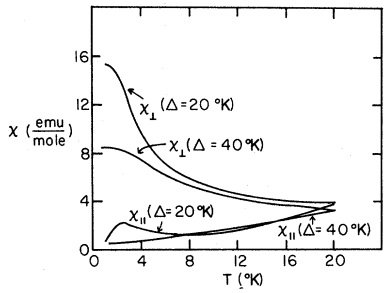

FIG. 6. Transverse and longitudinal susceptibilities for $T_N = 20$ °K with $\Delta = 20$ °K and $\Delta = 40$ °K. This illustrates the behavior in the regime where the susceptibility is most anomalous.

splitting with varying h_m similar to that of a simple $S=\frac{1}{2}$ system, and is expected to behave normally. For $\Delta = 200\ ^\circ\mathrm{K}$ and $T_N = 20\ ^\circ\mathrm{K}$, $h_m(T=0) = 36$ and we found a monotonic increase of $1/\chi$ as T decreases.

Finally, it is interesting to note that if the quartet crystal-field state is lower than the doublet, i.e., if B_4 is negative, then there is no level crossing of the two lowest levels. (This can be seen by inverting Fig. 1 with regard to energy.) The susceptibilities calculated then show no anomaly for all values of Δ.

V. APPLICATION TO CERIUM–GROUP-V COMPOUNDS

The magnetic susceptibilities of Ce–group-V compounds have been measured in powder (i.e., polycrystalline) samples by several workers.[2–5] Although the data of the different groups differ in detail, they show the same qualitative behavior. The susceptibilities of the lighter compounds CeP and CeAs behave anomalously in the paramagnetic phase, but normally below the Néel temperature. On the other hand, CeSb and CeBi show essentially no anomaly in the paramagnetic phase but strong anomalies in the ordered phase. In this section we discuss this behavior on the basis of our model.

A. CeP and CeAs

In the neutron diffraction experiments of Rainford *et al.*[8] the magnetic structure of CeAs has been identified as fcc type-I antiferromagnetic with moments pointing along the c axis. The same group of workers, using the neutron inelastic scattering technique, also determined the crystal-field splitting Δ between the ground-state doublet and the excited quartet as $(140 \pm 10)\ ^\circ\mathrm{K}$. This is in good agreement with the result $\Delta = (142 \pm 12)\ ^\circ\mathrm{K}$ obtained by Furrer *et al.*[9] CeP shows behavior very similar to that of CeAs. Assuming the same type-I magnetic structure, Jones[7] showed that the anomalous susceptibility behavior in the paramagnetic regime can be understood if there is a crystal-field splitting of about $200\ ^\circ\mathrm{K}$. The Néel temperatures of CeAs and CeP are 8 and $10\ ^\circ\mathrm{K}$, respectively. Accordingly, they correspond to the case where the crystal field is much greater than the exchange molecular field; and our discussion in Sec. IV shows that the susceptibility in the ordered state should behave normally.

To obtain the crystal-field splitting Δ involved in the calculation of susceptibility in the ordered phase, we took the measured $1/\chi$ values in the paramagnetic phase of each compound and performed a least-squares fit to the equation,

$$\chi_p^{-1} = (\chi_p^0)^{-1} - \Theta/C_M \ , \qquad (5.1)$$

where χ_p^0 (which depends on Δ) and C_M are given in Eqs. (3.15) and (3.16). Since the paramagnetic

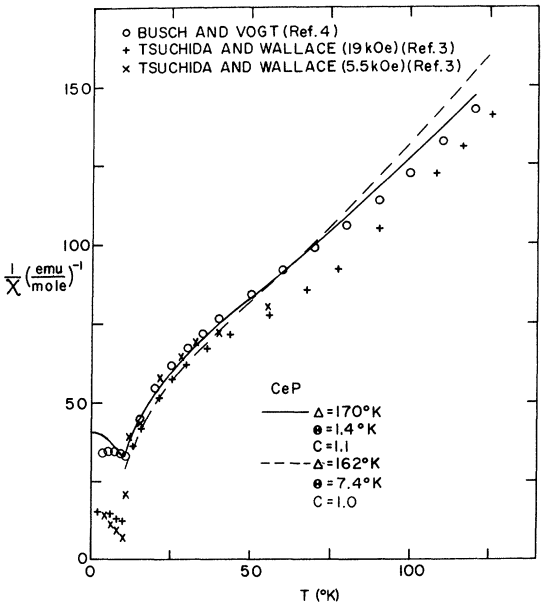

FIG. 7. Inverse susceptibility versus temperature for CeP. Three sets of data and two calculated curves are shown. The dashed line gives the best fit to the data of Busch and Vogt (denoted by circles) with $C = \chi_{\text{sample}}/\chi_f = 1$. The solid line is obtained by taking $C = 1.1$ as estimated using the reported value of μ_{eff}.

Curie temperature Θ could not be determined accurately, we used it as an additional parameter to fit the data. Assuming the same magnetic structure as that of CeAs, the best fit to the data of Busch and Vogt[4] for CeP was determined with $\Delta = 160\ ^\circ\mathrm{K}$ and $\Theta = 6.7\ ^\circ\mathrm{K}$. This is shown by the dashed curve in Fig. 7. The deviation of the experimental data from this theoretical curve is quite considerable. While the low-temperature points lie above the calculated curve, the high-temperature points fall under it. Even worse is the fact that the slope of the curve (almost a straight line) at high temperatures differs from the slope shown by the data points. This means that the $1/\chi$ data at higher temperatures than those shown in Fig. 7 will differ from the calculation by an even larger amount. This is partially due to the fact that the fit was done to $T = 120\ ^\circ\mathrm{K}$. On the other hand, however, if we could include all the higher-temperature data, say, up to room temperature, we would just make the low-temperature fit too poor to be accepted. *The same difficulties occurred in the* CeAs *data fit.* The main source of this discrepancy between the theory and the experiment may be due to: (i) The observed susceptibility actually contains several other contributions which the theory has not taken into account. Indeed, the s-f interaction could alter

the temperature-dependent susceptibility by as much as 10%.[7,10] The deviation of the measured effective moment (in the paramagnetic phase) from a free-ion moment is generally attributed to this effect. (ii) The experimental uncertainties could be large. This is reflected in the differences between the measurements of different groups shown in Fig. 7 for CeP and in Fig. 8 for CeAs.

To improve the fit, without knowing the details of the experimental uncertainty, we proceed to modify the theory to include the possible effect of s-f interaction enhancement of the susceptibility estimated from the experimental measurements.

Noting that the susceptibility is proportional to μ_{eff}^2, we multiply the calculated f-electron susceptibility by a factor C,

$$C = (\mu_{eff}/\mu_{free})^2 . \qquad (5.2)$$

If we take the reported value of μ_{eff} in each experiment to determine the value of C, we can obtain a reasonable fit of the measurements.

For CeP, we took the measurement of Busch and Vogt[4] and the best fit to the data points in the paramagnetic phase gives the crystal-field splitting $\Delta = 170\ ^\circ\mathrm{K}$ and the paramagnetic Curie temperature $\Theta = 1.4\ ^\circ\mathrm{K}$ for $C = 1.1$ ($\mu_{eff} = 2.66\mu_B$,[4] $\mu_{free} = 2.54\mu_B$). This is shown as the solid curve in Fig. 7. Using this set of parameters to calculate the susceptibility in the antiferromagnetically ordered state, we found a much steeper increase of the inverse susceptibility as T decreases than did Busch and Vogt.[4] However, the qualitative nature of the calculated behavior agrees quite well with the steeply increasing $1/\chi$, for T decreasing below T_N, found in the low field (5.5 kOe) measurements of Tsuchida and Wallace.[3] We note that the higher field (19 kOe) measurements of Tsuchida and Wallace show a flat temperature dependence below T_N. This suggests that the disagreement with the Busch-Vogt data may arise from those measurements being done at a relatively high field. Unfortunately, the data of Tsuchida and Wallace show a sharp drop in $1/\chi$ at T_N. This does not appear in the data of Busch and Vogt, nor can it be understood in the present theory.

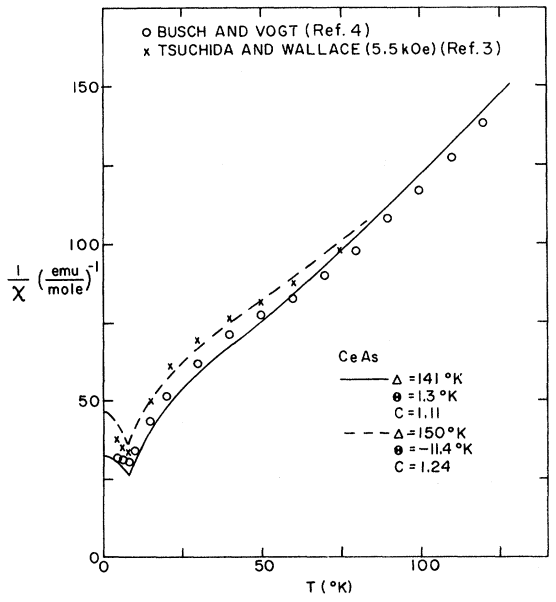

FIG. 8. Inverse susceptibility versus temperature for CeAs. The dashed line is the best fit to the data of Tsuchida and Wallace with $C = 1.24$ and the solid line gives the best fit to the data of Busch and Vogt with $C = 1.11$.

A fit to the measurements of CeAs has been carried out in the same way. In Fig. 8, we show the fit of two sets of experimental points in the paramagnetic phase. The obtained parameters, Δ and Θ, for each case are then used to construct the corresponding curve in the ordered region. From the measurement of Busch and Vogt,[4] $\mu_{eff} = 2.67$, so $C = 1.11$, and the parameters which give the best fit are

Busch and Vogt:

$$\Delta = 141\ ^\circ\mathrm{K}, \quad \Theta = 1.3\ ^\circ\mathrm{K} \quad (C = 1.11) .$$

On the other hand, taking the data of Tsuchida and Wallace (done at low magnetic field 5.5 kOe) and the reported value of effective moment $\mu_{eff} = 2.82$, we obtain $C = 1.24$, and the parameters are

Tsuchida and Wallace:

$$\Delta = 150\ ^\circ\mathrm{K}, \quad \Theta = -11.4\ ^\circ\mathrm{K} \quad (C = 1.24) .$$

Both fits in the paramagnetic regime are reasonably good. Again, the behavior of inverse susceptibility in the ordered region agrees only with the low magnetic field measurement.

B. CeSb and CeAs

For CeSb and CeBi the susceptibility measurements in the paramagnetic regime show essentially no deviation from Curie-Weiss behavior down to their respective ordering temperatures. This indicates a much smaller crystal-field splitting than in CeP or CeAs. For CeSb this has been confirmed by neutron inelastic scattering[8] which shows a splitting about 25 °K. We also expect a small crystal-field splitting in CeBi. The ordering temperatures of CeSb and CeBi are 16 and 25 °K, respectively. Thus CeSb and CeBi are cases where Δ is about equal to or less than kT_N, and we expect anomalies in the susceptibilities for the ordered phase.

Unfortunately, the magnetic structures of CeSb

and CeBi are not known in detail. However, neutron diffraction[8,11] indicates that the structures may be noncollinear. For CeSb, a further complication arises from the lattice distortion[12] at ordering and the effects of such distortion on the exchange interaction in the ordered phase.

Without more information on the magnetic structures of CeSb and CeBi a detailed quantitative analysis is impossible. Our discussion here is therefore confined to a qualitative basis.

Assuming a collinear magnetic structure with spins parallel to the direction of tetragonal distortion, we present a comparison of the theory and the experimental results for CeSb in Fig. 9. We have used a least-square fit to the data taken by Tsuchida and Wallace[3,14] in the ordered phase at low magnetic field to determine the parameters of the theory. Here it is important to use only the measurement done at low magnetic field (2.1 kOe) because of the metamagnetic transition observed at ~5 kOe.[15] Restricting Δ, the cubic crystal-field splitting, to have an upper bound of 30 °K, the following additional parameters were allowed to vary: δ, the relative size of second-order crystal-field potential as defined in Eq. (2.5); Θ', the paramagnetic Curie temperature in the distorted phase; and T'_N, the Néel temperature in the distorted phase. The best fit shown in Fig. 9 is obtained with

CeSb: $\Delta = 30\ ^\circ\mathrm{K}$, $\delta = -3.5$, $\Theta' = 8.6\ ^\circ\mathrm{K}$, $T'_N = 35\ ^\circ\mathrm{K}$.

We note that the value of δ is comparable to the value -1.72 calculated from a point charge model with the distortion measured by Levy.[12] T'_N would be the ordering temperature if the crystal remained tetragonal in the paramagnetic phase. However, this is not the case, and the measured Néel temperature is therefore lower.

We also note that the calculation shown in Fig. 9 was not able to reproduce the upturned tail of the experimental curve below 7 °K. This failure may rest on one of the effects neglected in the calculation: first, the possible effect of a noncollinear magnetic structure; second, the likely importance of the exchange striction, i.e., the molecular field constant λ is a function of the lattice parameter. An increase of λ with increasing distortion at lower temperature (observed by Levy[12]) would give an upturn in $1/\chi$.

In the paramagnetic regime, the theoretical curve for $\Delta = 30\ ^\circ\mathrm{K}$, $\Theta = 5\ ^\circ\mathrm{K}$ lies above the experimental points at lower temperatures and has more curvature than is indicated by the experimental points of Tsuchida and Wallace as reproduced in Fig. 9. This may indicate that the crystal-field splitting is smaller in the paramagnetic phase. [In Fig. 9 we have included a $\Delta = 20\ ^\circ\mathrm{K}$, $\Theta = 5\ ^\circ\mathrm{K}$ curve (dashed line) in the paramagnetic regime to show the effect of such a decrease. Such a decrease in Δ could be associated with the absence of lattice distortion in the paramagnetic phase.] Alternatively, the curvature of the experimental $1/\chi$ may be greater than that indicated by the data of Tsuchida and Wallace shown. (Vogt's recent data[14] shows the possibility of significant curvature in $1/\chi$ just above T_N.)

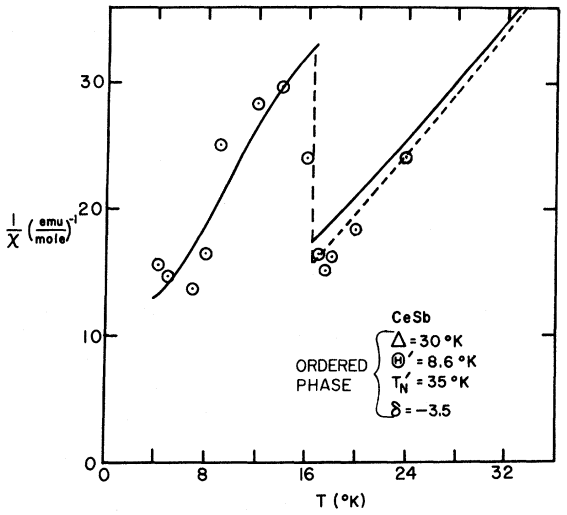

FIG. 9. Inverse susceptibility versus temperature for CeSb. Experimental data are those of Tsuchida and Wallace (2.1 kOe). Parameters used in the calculation in the ordered regime are $\Delta = 30\ ^\circ\mathrm{K}$, $\delta = -3.5$, $\Theta' = 8.6\ ^\circ\mathrm{K}$, $T'_N = 35\ ^\circ\mathrm{K}$. In the paramagnetic regime we show two curves, the solid curve with $\Delta = 30\ ^\circ\mathrm{K}$, $\Theta = 5\ ^\circ\mathrm{K}$ and the dashed curve with $\Delta = 20\ ^\circ\mathrm{K}$, $\Theta = 5\ ^\circ\mathrm{K}$.

For CeBi we have even less information. Because of the fact that metamagnetic transition occurs at ~10 kOe[16] and because of the observation of the hysteresis effect[2] after applying a magnetic field to the sample, we choose to fit the data taken by Tsuchida and Wallace[2] *in the ordered phase* at low field (5.5 kOe) and for the virgin material only. Assuming an fcc lattice without distortion and a type-I antiferromagnet, we found it impossible to fit the data with isotropic exchange interaction between two spins. However, with two paramagnetic molecular field constants, the fitting is surprisingly good, as shown in Fig. 10. The set of parameter giving the best fit is $\Delta = 21\ ^\circ\mathrm{K}$, $\bar{\lambda}_u = 6.6\ (\mathrm{emu/mole})^{-1}$, and $\bar{\lambda}_\perp = -6.0\ (\mathrm{emu/mole})^{-1}$ (with $\bar{\lambda}$ defined in Sec. III). Although the exchange interaction being anisotropic is plausible,[17,18] further experiments (such as susceptibility measurements on single crystal) are needed to confirm this fact.

Finally, it is worth mentioning that the level crossing effects described above, together with successive lattice distortions, certainly play a key

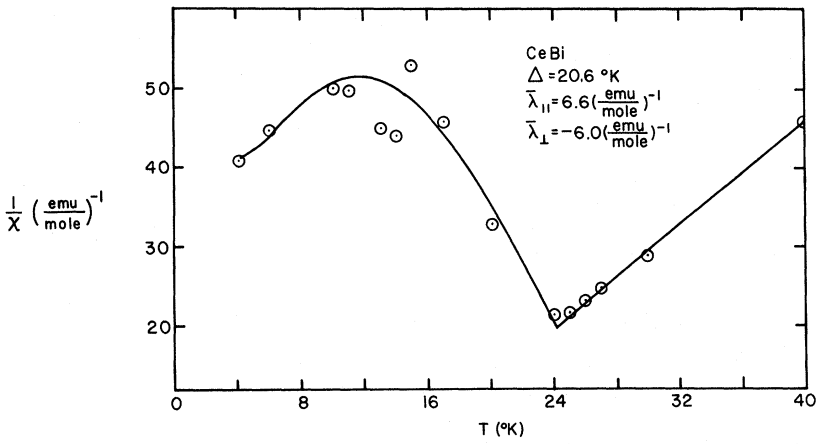

FIG. 10. Inverse susceptibility versus temperature for CeBi. Experimental data are those of Tsuchida and Wallace (5.5 kOe, virgin sample). Anisotropic exchange is assumed in the calculation. The parameters are $\Delta = 20.6\,°K$, $\bar{\lambda}_{\parallel} = 6.6$ (emu/mole)$^{-1}$, $\bar{\lambda}_{\perp} = -6.0$ (emu/mole)$^{-1}$.

role in the occurrence of the remarkable sharp steps[15] in the magnetization versus applied field behavior for single crystals of CeSb at 1.5 °K, and the similar behavior for CeBi powder.[16] Both for understanding these effects and for a detailed quantitative theory of the $1/\chi$ versus T behavior of "real" CeSb, detailed knowledge of the magnetic structure such as would be found by neutron diffraction is highly desirable. Such experiments done including applied field effects on single crystals would be especially valuable.

ACKNOWLEDGMENTS

We would like to thank Professor W.E. Wallace, Professor W.G. Moulton, and Professor W. Wolf for interesting discussions. One of us (Y.L.W.) enjoyed the hospitality of the General Electric Research and Development Center during a summer's visit.

---

*Research partially sponsored by the Air Force Office of Scientific Research, Office of Aerospace Research, USAF, under Grant No. AFOSR-69-1745.

[1]We have previously discussed the induced moment effects on magnetic order for a non-Kramers ion where the crystal-field ground state can be a singlet: B. R. Cooper, Phys. Rev. 163, 444 (1967); Y. L. Wang and B. R. Cooper, *ibid.* 172, 539 (1968); 185, 696 (1969); B. R. Cooper, J. Appl. Phys. 40, 1344 (1969).

[2]T. Tsuchida and W. E. Wallace, J. Chem Phys. 43, 2087 (1965).

[3]T. Tsuchida and W. E. Wallace, J. Chem. Phys. 43, 2885 (1965). *Note necessary correction to the ordinate scale in* Fig. 3 *of this paper giving* $1/\chi$ *of* CeP. We are grateful to Professor W. E. Wallace for providing the correct data.

[4]G. Busch and O. Vogt, Phys. Letters. 20, 152 (1966).

[5]T. Tsuchida and Y. Nakamura, J. Phys. Soc. Japan 25, 284 (1968).

[6]K. A. Gschneider, Jr., *Rare Earth Alloys* (Van Nostrand, Princeton, 1961), p. 375.

[7]E. D. Jones, Phys. Letters 22, 266 (1966).

[8]B. Rainford, K. C. Turberfield, G. Busch, and O. Vogt, J. Phys. C 1, 679 (1968).

[9]A. Furrer, W. Halg, and T. Schneider, *Neutron Inelastic Scattering* (International Atomic Energy Agency, Vienna, 1968), Vol. II, pp. 133–139.

[10]E. D. Jones, Phys. Rev. 180, 455 (1969).

[11]L. M. Corliss and J. M. Hastings (private communication); and quotation of Corliss and Hastings in Ref. 2.

[12]Such a distortion has been observed by P. Levy, and we are grateful to Dr. Levy for making his data available to us (private communication); also, F. Levy, Physik Kondensierten Materie 10, 85 (1969).

[13]J. S. Smart, *Effective Field Theories of Magnetism* (Saunders, Philadelphia, 1966).

[14]Recent low field (3 kOe) measurements by Vogt show the same qualitative behavior as the data of Tsuchida and Wallace (shown in Fig. 9) and of Tsuchida and Nakamura (Ref. 3). However, Vogt obtains somewhat larger values of $1/\chi$ at the peak and a more pronounced upturn in $1/\chi$ at low T; O. Vogt (private communication).

[15]G. Busch and O. Vogt, Phys. Letters. 25A, 499 (1967).

[16]T. Tsuchida and Y. Nakamura, J. Phys. Soc. Japan 22, 942 (1967).

[17]J. H. Van Vleck, Rev. Mat. Fis. Teor. (Tucuman, Argentina) 14, 189 (1962).

[18]To have a net anisotropic contribution to the exchange field in molecular field theory for a cubic material requires having a biquadratic, or higher degree exchange [P. R. Cooper and O. Vogt, Phys. Rev. B 1, 1218 (1970)]. However, the essential qualitative effects of such an anisotropic exchange can probably be included by our simple approximation of using an anisotropic coefficient for the linear molecular field.